

# Stress-compatible embedded cohesive crack in CST element

J.F. Olesen & P.N. Poulsen

*Technical University of Denmark, Denmark*

**ABSTRACT:** A simple element with an embedded strong discontinuity for modeling cohesive cracking of concrete is presented. The element differs from previous elements of the embedded type, in that a consistent stress field is obtained by direct enforcement of stress continuity across the crack. The displacement discontinuity is modeled in an XFEM fashion; however, the discontinuous displacement field is special, allowing for the direct enforcement of stress continuity. This in turn allows for elimination of extra degrees of freedom necessary for describing the crack deformations, thus the element has the same number of freedoms as its continuous basis: CST. The good performance of the element is demonstrated by its ability to simulate three-point bending of a notched concrete beam. The advantage of the element is its simplicity and the straightforward implementation of it. Handling situations with multiple cracks will not require further developments, although this is not demonstrated here.

## 1 INTRODUCTION

The 2D modeling of concrete cracking in the framework of FEM has already reached an advanced level, and developments in this field over the past decade have been characterized as XFEM, the eXtended Finite Element Method, see (Belytschko & Black 1999), (Moës et al. 1999) and (Moës & Belytschko 2002). For refinements of the method applied to cohesive cracking allowing for partly cracked elements, see (Asferg et al. 2007) and (Mougaard et al. 2009). Although these methods are very effective, the drawback, however, is that it takes a lot of bookkeeping, at the system level as well as at the element level, to ensure conformity and to model separation of the discontinuous parts of an element accurately, i.e. in such a way that it allows for fully independent deformations of the two separated parts.

The element which is proposed here is a 2D element of the embedded discontinuity type with a strong discontinuity; this embedded discontinuity type was originally introduced by (Dvorkin, E.N. et al. 1990). Further developments were presented by (Oliver 1996); this work is based on the assumed enhanced strain approach and differs from the present work in that it does not enforce stress continuity directly, but in a variational manner.

The advantage of the embedded element type is that it is simple to implement and that it does not complicate the building of the FE system Equation. The drawbacks of it is that it lacks the ability to create completely independent element separations and that displacement continuity is violated on element

sides crossed by a crack; however, in many cases these deficiencies might be considered to be of minor importance.

The present element takes advantage of the systematic construction of displacement fields in XFEM, except that the discontinuous shape functions are not the same as the continuous. Besides from being of the embedded type the present element is characterized by having a consistent stress field which is continuous across the discontinuity. Enforcing this stress continuity in the element we obtain the possibility of eliminating the extra degrees of freedom (DOF) necessary for describing the discontinuity; hereby an element is realized with no extra DOF's compared to the continuous version of the element.

The present element allows for cohesive cracking with a stress criterion for crack initiation, i.e. a crack initiates if the uni-axial tensile strength is exceeded by the first principle stress and no stress intensity is assumed at the crack tip, assuming smooth crack closure.

## 2 KINEMATICS

The modeling of a strong discontinuity, such as a crack, is based on the strategy of the extended finite element method for the approximation of a displacement fields with a discontinuity. Thus, the displacement field approximation in an element with a discontinuity is established by combining the displacement field corresponding to the continuous element with the displacement field corresponding

to the discontinuity.

For the linear interpolation of the continuous displacement field we consider a three-node triangular element, the CST. The element is given the possibility of a strong discontinuity along a straight line crossing the element. The enforcement of stress compatibility between the stresses in the continuous parts of the element and the stresses bridging the discontinuity line is the essential idea of the present work. Stress compatibility is ensured by demanding that the order of variation of the discontinuous displacement fields along the discontinuity line must match the order of variation of the continuous stress fields, and that the discontinuous displacement field produces equal stresses on opposite sides of the discontinuity. In the case of a CST this leads to a displacement field with a constant jump in the displacement along the discontinuity line, which will produce constant bridging stresses along the discontinuity matching the constant stress field of the CST. Further, this displacement field must produce equal gradients on either side of the discontinuity.

A shape function that allows for a constant jump across a straight line and at the same time only introduces equal and constant strains on either side of the discontinuity line is shown in Figure 1. The shape function may be written in terms of the natural coordinate  $\zeta$  associated with the element vertex which is also a vertex of the triangular sub-domain  $\Omega_e^-$ :

$$N^d = \begin{cases} \zeta - 1 & \text{in } \Omega_e^- \\ \zeta & \text{in } \Omega_e^+ \end{cases} \quad (1)$$

This type of shape function has previously been applied by (Oliver 1996). Only two DOF's are needed to describe the discontinuous deformations. We chose the global components of the discontinuity vector and collect these DOF's in the vector  $\mathbf{V}^d = [\Delta V_1, \Delta V_2]^T$ . Each DOF is associated with a discontinuous shape function as given in (1), and the discontinuous displacement field vector  $\mathbf{u}^d$  is introduced as

$$\mathbf{u}^d = \mathbf{N}^d \mathbf{V}^d, \quad \mathbf{N}^d = \begin{bmatrix} N^d & 0 \\ 0 & N^d \end{bmatrix} \quad (2)$$

By combining  $\mathbf{u}^d$  with the continuous displacement field vector  $\mathbf{u}^c = \mathbf{N}^c \mathbf{V}^c$  for the normal CST element we arrive at the total deformation field:

$$\mathbf{u} = \mathbf{u}^c + \mathbf{u}^d = \mathbf{N}^c \mathbf{V}^c + \mathbf{N}^d \mathbf{V}^d \quad (3)$$

where  $\mathbf{N}^c$  is the usual linear interpolation matrix and  $\mathbf{V}^c$  the usual *dof* vector.

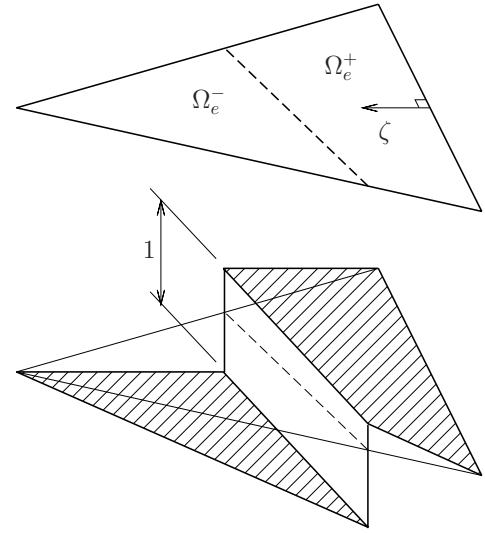


Figure 1. *Top*: Straight discontinuity line defining element sub-domains, and the associated natural coordinate  $\zeta$ .

*Bottom*: Illustration of constant discontinuity shape function.

Adopting the Voigt notation and assuming a linear strain measure, the strains in the continuous part of the element may be written as the vector

$$\boldsymbol{\varepsilon} = \mathbf{B}^c \mathbf{V}^c + \mathbf{B}^d \mathbf{V}^d \quad (4)$$

where  $\mathbf{B}^c$  is the usual constant strain interpolation matrix and  $\mathbf{B}^d$  is the constant strain interpolation matrix derived from the discontinuous shape function. Note that  $\mathbf{B}^d$  is the same on both sides of the discontinuity.

### 3 VARIATIONAL AND FEM FORMULATIONS

Consider a linear elastic body in a state of plane stress or plane strain. The body is situated in a plane Cartesian coordinate system  $(x_1, x_2)$ . Assume that a crack has formed in the body, see Figure 2. The unit tangent vector to the curvilinear crack path is denoted by  $\mathbf{s}$ , and the normal to the crack path is denoted by  $\mathbf{n}$ . At any point along the crack  $(n, s)$  defines a local right-hand coordinate system. The negative side of the crack is defined as the side where  $\mathbf{n}$  coincides with the outward normal to the crack face. The stress transfer over the crack is given as the normal and tangential tractions,  $\sigma_n$  and  $\tau_{ns}$ , respectively. These are the generalized stresses in the crack, and their work-conjugate generalized strains are the normal opening of the crack,  $\Delta u_n = u_n^+ - u_n^-$ , and the tangential slip of the crack faces,  $\Delta u_s = u_s^+ - u_s^-$ . The generalized stresses and strains in the crack are collected in vectors according to

$$\boldsymbol{\sigma}^{cr} = \begin{Bmatrix} \sigma_n \\ \tau_{ns} \end{Bmatrix}, \quad \llbracket \mathbf{u} \rrbracket = \begin{Bmatrix} \Delta u_n \\ \Delta u_s \end{Bmatrix} \quad (5)$$

where  $\llbracket \mathbf{u} \rrbracket$  signifies a jump in the displacement field  $\mathbf{u}$  related to the local  $(n, s)$  coordinate system.

The stresses bridging the crack are typically functions of the crack opening and sliding as well as of the history of opening and sliding. At this point we assume that the bridging stresses may be written as a function of  $\llbracket \mathbf{u} \rrbracket$ :

$$\boldsymbol{\sigma}^{cr} = \boldsymbol{\sigma}^{cr}(\llbracket \mathbf{u} \rrbracket) \quad (6)$$

The internal virtual work  $\delta W^I$  and the external virtual work  $\delta W^E$  may be stated as

$$\delta W^I = \int_{\Omega} \delta \boldsymbol{\varepsilon}^T \boldsymbol{\sigma} d\Omega + \int_S \delta \llbracket \mathbf{u} \rrbracket^T \boldsymbol{\sigma}^{cr} dS \quad (7)$$

$$\delta W^E = \int_{\Omega} \delta \mathbf{u}^T \mathbf{f} d\Omega + \int_{\Gamma_t} \delta \mathbf{u}^T \bar{\mathbf{t}} d\Gamma \quad (8)$$

where  $\boldsymbol{\sigma}$  and  $\boldsymbol{\varepsilon}$  are the work conjugate stress and strain vectors,  $\mathbf{f}$  is the domain load vector,  $\bar{\mathbf{t}}$  is the prescribed boundary traction vector, and the prefix  $\delta$  denotes the variation of the subsequent field.

The un-cracked bulk material is assumed to be linear elastic and constitutive Equation is written in the form

$$\boldsymbol{\sigma} = \mathbf{D}\boldsymbol{\varepsilon} \quad (9)$$

where  $\mathbf{D}$  is the appropriate material stiffness matrix.

Stress compatibility across the discontinuity is ensured by demanding the traction  $\mathbf{t}^{cr}$  on the crack faces to equal the bridging stresses

$$\mathbf{T}^{cr} \mathbf{t}^{cr} = \boldsymbol{\sigma}^{cr} \quad (10)$$

where  $\mathbf{T}^{cr}$  is a transformation matrix depending on the orientation of the crack. The traction may be determined from

$$\mathbf{t}^{cr} = \mathbf{m}\boldsymbol{\sigma}, \quad \mathbf{m} = \begin{bmatrix} n_1 & 0 & n_2 \\ 0 & n_2 & n_1 \end{bmatrix} \quad (11)$$

where  $\mathbf{m}$  is a matrix based on the elements of the normal vector of the crack face  $\mathbf{n} = (n_1, n_2)$ . Introducing into (6), (10) and (11) the element field approximations (4) and (9), and utilizing that  $\llbracket \mathbf{u} \rrbracket = \mathbf{T}^{cr} \mathbf{V}^d$  the stress compatibility requirement may be expressed at the element level as

$$\mathbf{T}^{cr} \mathbf{m} \mathbf{D} [\mathbf{B}^c \mathbf{V}^c + \mathbf{B}^d \mathbf{V}^d] = \boldsymbol{\sigma}^{cr} (\mathbf{T}^{cr} \mathbf{V}^d) \quad (12)$$

The nature of this Equation depends on (6), and in general it is nonlinear in  $\mathbf{V}^d$ . However, it may be solved for  $\mathbf{V}^d$  at the element level, thus allowing

for the elimination of the DOF's describing the discontinuity. The variation of  $\mathbf{V}^d$  may be established by taking the variation of (12):

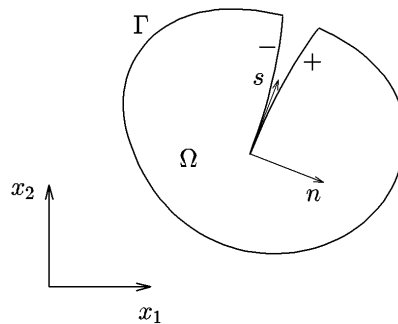


Figure 2. Global coordinate system  $(x_1, x_2)$  and local crack coordinate system  $(n, s)$ .

$$\mathbf{T}^{cr} \mathbf{m} \mathbf{D} [\mathbf{B}^c \delta \mathbf{V}^c + \mathbf{B}^d \delta \mathbf{V}^d] = \frac{\partial \boldsymbol{\sigma}^{cr}}{\partial \llbracket \mathbf{u} \rrbracket} \frac{\partial \llbracket \mathbf{u} \rrbracket}{\partial \mathbf{V}^d} \delta \mathbf{V}^d \quad (13)$$

We introduce  $\mathbf{D}^{cr}$  as the generalized tangential stiffness of the crack bridging, i.e.

$$\mathbf{D}^{cr} = \frac{\partial \boldsymbol{\sigma}^{cr}}{\partial \llbracket \mathbf{u} \rrbracket} \quad (14)$$

Realizing that  $\partial \llbracket \mathbf{u} \rrbracket / \partial \mathbf{V}^d = \mathbf{T}^{cr}$ , the variation of  $\mathbf{V}^d$  may be isolated from (13) in the form

$$\delta \mathbf{V}^d = \mathbf{Z} \delta \mathbf{V}^c \quad (15)$$

where

$$\mathbf{Z} = [\mathbf{D}^{cr} \mathbf{T}^{cr} - \mathbf{T}^{cr} \mathbf{m} \mathbf{D} \mathbf{B}^d]^{-1} \mathbf{T}^{cr} \mathbf{m} \mathbf{D} \mathbf{B}^c \quad (16)$$

The approximation to the internal virtual work in an element may now be expressed by

$$\delta W^I = \delta \mathbf{V}^{cT} \left[ \int_{\Omega} [\mathbf{B}^{cT} + \mathbf{Z}^T \mathbf{B}^{dT}] \boldsymbol{\sigma} d\Omega + \int_S \mathbf{Z}^T \mathbf{T}^{crT} \boldsymbol{\sigma}^{cr} dS \right] \quad (17)$$

where all quantities now relate to an element. The stresses that enter into this expression are determined as:

$$\boldsymbol{\sigma} = \mathbf{D} [\mathbf{B}^c \mathbf{V}^c + \mathbf{B}^d \mathbf{V}^d] \quad (18)$$

$$\boldsymbol{\sigma}^{cr} = \boldsymbol{\sigma}^{cr} (\mathbf{T}^{cr} \mathbf{V}^d) \quad (19)$$

Equation (17) constitutes the element nodal force vector  $\mathbf{q}$  such that we may write  $\delta W^I = \delta \mathbf{V}^{cT} \mathbf{q}$ .

The differential form of the internal virtual work reads

$$d\delta W^I = \int_{\Omega} \delta \boldsymbol{\varepsilon}^T d\boldsymbol{\sigma} d\Omega + \int_S \delta \llbracket \mathbf{u} \rrbracket^T d\boldsymbol{\sigma}^{cr} dS \quad (20)$$

In an element this may be expressed solely in terms of the usual (continuous) DOF vector  $V^c$ :

$$d\delta W^I = \delta V^{cT} \left[ \int_{\Omega} [B^{cT} + Z^T B^{dT}] D [B^c + B^d Z] d\Omega + \int_S Z^T T^{crT} D^{cr} T^{cr} Z dS \right] dV^c \quad (21)$$

This Equation constitutes the element stiffness matrix  $k_T$  such that we may write  $d\delta W^I = \delta V^{cT} k_T dV^c$ . The tangent stiffness matrix is only symmetric if the matrix  $D^{cr}$  is symmetric, which is not necessarily the case. However, for iterative purposes  $D^{cr}$  may be replaced by the symmetric matrix  $\frac{1}{2}[D^{cr} + D^{crT}]$ .

#### 4 NUMERICS

On the global level the virtual work Equation furnishes the discrete equilibrium Equation:

$$Q(V) = R \quad (22)$$

where  $Q$  is the sum of element nodal forces established through Equations (17)-(19),  $V$  is the global DOF vector and  $R$  is the global nodal load vector determined from (8). Equation (22) is a set of nonlinear Equation which are solved iteratively applying the linear incremental relation

$$K_T dV = dR \quad (23)$$

where  $K_T$  is the global tangent stiffness matrix assembled from element matrices established through (21),  $dV$  is the global incremental DOF vector and  $dR$  is global incremental load vector.

The element presented in the previous section is based on the CST, however, it allows for the formation of a displacement discontinuity or a crack. Thus we have named the element ‘‘dCST’’. The dCST has three nodes and six DOF’s, two at each node describing the displacement vector. The actual value of the discontinuity vector is calculated at the element level and no global DOF’s are needed to represent these vector elements.

A crack is formed if the principle stress in an element exceeds the uni-axial tensile strength, and the normal to the discontinuity line is parallel to the principle stress vector. If a neighboring element is in the cracked state, the crack in the actual element is forced to connect to the neighboring crack; otherwise it is forced to pass through the center of the element.

The nonlinear equilibrium Equation may be solved by standard FEM procedures; here we have applied the orthogonal residual algorithm (Krenk 1995). Convergence is ensured at every load step in

terms of an energy criterion related to the elastic energy of the initial elastic load step.

#### 5 EXAMPLE

The capabilities of the dCST element are demonstrated through the modeling of the RILEM three-point bending test (Vandervalle 2000) for determining fracture mechanical properties of concrete, which has become a benchmark test also for the numerical modeling of cohesive fracture propagation. A side view of the test setup is shown in Figure 3. The beam has a square cross-section and a 25 mm deep notch cut perpendicular to the bottom face in the mid-section plane; it is simply supported at the ends and loaded by a load acting vertically downwards at mid-span.

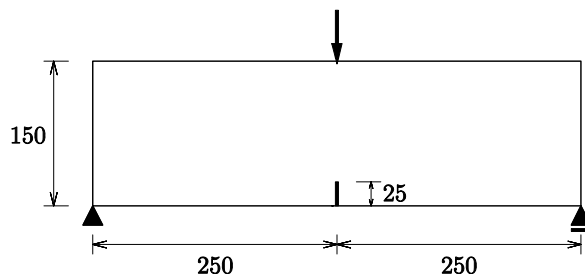


Figure 3. Geometry of the RILEM test beam with a 25 mm notch.

The beam is assumed to be cast in concrete with characteristics according to Table 1. The tensile softening of the concrete is assumed to obey a linear cohesive law as depicted in Figure 4. The crack propagation in this test is dominated by the opening of the crack, hence the mixed mode characteristics of the concrete are not considered. However, sliding of the crack faces must produce some stress in order to avoid unrestricted rigid body motion of the cracked element part which is only attached to one node. Therefore, sliding is modeled elastically with an inferior stiffness. No interaction between the two crack deformations is considered.

Table 1. Concrete material parameters.

Parameter	Value
Young’s modulus, $E_c$	37.4 GPa
Poisson’s ratio, $\nu_c$	0.2
Tensile strength, $f_t$	3.5 MPa
Fracture energy, $G_f$	160 J/m <sup>2</sup>

The dCST element is tested against the performance of an interface element supplied with the commercially available FEM code DIANA (Diana 2003). In the DIANA reference model the bulk of the beam is modeled with CST elements, and inter-

face elements are pre-located to model a crack path confined to the mid-span section of the beam.

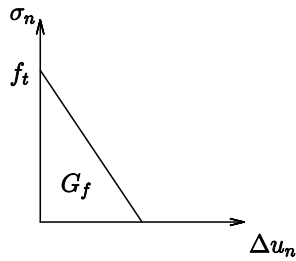


Figure 4. Linear tension softening curve.

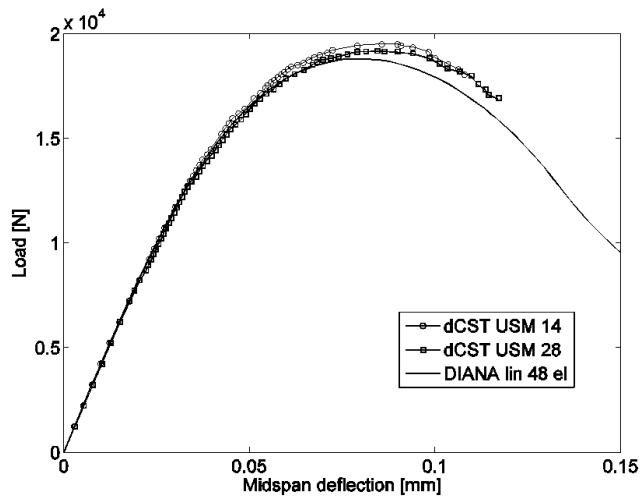


Figure 5. Load-deflection curves of the RILEM test beam with a 25 mm notch. Comparison between a DIANA model with 48 interface elements over the ligament height, and two dCST models with unstructured meshes having 14 and 28 elements over the ligament height, respectively.

To make a fair comparison between the dCST model and the reference model, the dCST model is allowed to develop one crack only, although it has the capability of modeling multi crack development. The one-crack restriction is obtained by only allowing an element to crack if it has a neighbor which is cracked. However, to get starting, the first element to crack is exempted from this rule.

The reference beam was modeled in a regular mesh with 48 elements over the height of the beam. Unstructured meshes were used for the dCST-models with two densities furnishing 14 and 28 elements over the ligament height, respectively.

Simulated load-deflection curves are shown in Figure 5. The deflection is measured at mid-span relative to the mean value of the deformations of the beam mid-plane at the supports. Results for both meshes compare nicely with the results for the reference model, although the dCST model slightly overestimates the peak load. It should be emphasized, though, that the crack path has not been predefined in the dCST models. In Figure 6 the element meshes close to the notch and crack paths at peak load are shown, respectively for the two mesh densities applied. Only the middle part of the beam ( $\pm 25$ mm

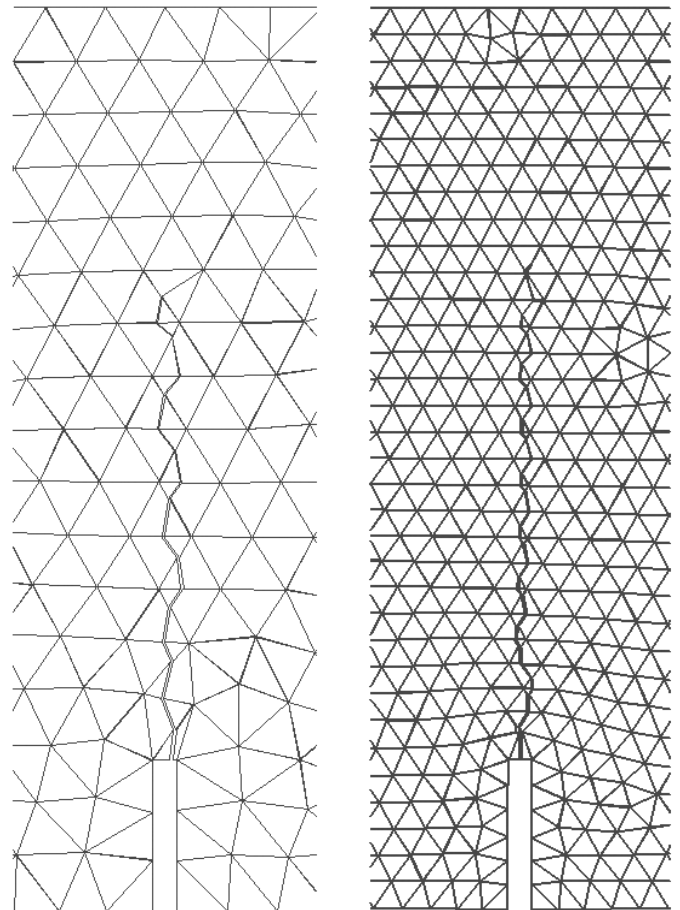


Figure 6. Element mesh for dCST model close to the notch, and crack path at peak load. The middle part of the beam ( $\pm 25$ mm from the mid-section) is shown for two mesh densities.

from the mid-section) is shown. The winding of the dCST cracks is of course a consequence of the coarse constant strain fields of the elements. However, the overall direction of the cracks is in line with the mid-section plane.

## 6 CONCLUSION

A simple element called dCST with an embedded discontinuity for modeling concrete cracking has been presented. The element differs from previous strong discontinuity elements of the embedded or XFEM type, in that the stress field is consistent within the element ensuring stress continuity across the crack. The direct enforcement of stress compatibility has allowed for the elimination of extra DOF's for describing the crack opening and sliding, thus the dCST has the same number of DOF's as the CST.

The good performance of the dCST has been demonstrated in the Mode I benchmark test: the three-point bending of a notched concrete beam.

The advantage of the dCST element is the simplicity of it. Implementation is straightforward and the handling of a multiple crack situation will not require further developments.

## REFERENCES

- Asferg, J.L., Poulsen, P.N. and Nielsen, L.O. 2007. A consistent partly cracked XFEM element for cohesive crack growth. *Int. J. Numer. Meth. Engng.* Vol. 72: 464-485.
- Belytschko, T. and Black, T. 1999. Elastic crack growth in finite elements with minimal remeshing. *Int. J. Numer. Meth. Engng.* Vol. 45: 601-620.
- Diana User Manual 2003. DIANA User Manual, Element Library, (Edition 8.1). TNO Building and Construction Research, Delft, The Netherlands.
- Dvorkin, E.N., Cuitiño, A.M. and Gioia, G. 1990. Finite elements with displacement interpolated embedded localization lines insensitive to mesh size and distortions. *Comp. Meth. in Appl. Mech. and Engng.* Vol. 90: 829-844.
- Krenk, S. 1995. An orthogonal residual procedure for nonlinear finite element equations. *Int. J. Numer. Meth. Engng.* Vol. 38: 823-839.
- Moës, N., Dolbow, J. and Belytschko, T. 1999. A finite element method for crack growth without remeshing. *Int. J. Numer. Meth. Engng.* Vol. 46: 131-150.
- Moës, N., and Belytschko, T. 2002. Extended finite element method for cohesive crack growth. *Engng. Fract. Mech.* Vol. 63: 276-289.
- Mougaard, J.F., Poulsen, P.N. and Nilesen, L.O. 2009. A partly and fully cracked XFEM element based on higher order polynomial shape functions for modeling cohesive fracture. Submitted for publication.
- Oliver, J. 1996. Modelling strong discontinuities in solid mechanics via strain softening constitutive equations. Part 1: Fundamentals. Part 2: Numerical simulation. *Int. J. Numer. Meth. Engng.* Vol. 39: 3575-3623.
- Vandervalle, L. 2000. Test and design methods for fiber reinforced concrete. Recommendations for bending test. *Mater. & Struct.* Vol. 33: 3-5.